

January 01, 2008

Mechanical and electrical evaluation of parylene-C encapsulated carbon nanotube networks on a flexible substrate

Chia-Ling Chen

Northeastern University - Dept. of Electrical and Computer Engineering

Ernesto Lopez

Northeastern University - Dept. of Mechanical and Industrial Engineering

Yung-Joon Jung

Northeastern University - Dept. of Mechanical and Industrial Engineering

Sinan Müftü

Northeastern University - Dept. of Electrical and Computer Engineering

Selvapraha Selvarasah

Northeastern University - Dept. of Electrical and Computer Engineering

See next page for additional authors

Recommended Citation

Chen, Chia-Ling; Lopez, Ernesto; Jung, Yung-Joon; Müftü, Sinan; Selvarasah, Selvapraha; and Dokmeci, Mehmet R., "Mechanical and electrical evaluation of parylene-C encapsulated carbon nanotube networks on a flexible substrate" (2008). *Center for High-Rate Nanomanufacturing Publications*. Paper 1. <http://hdl.handle.net/2047/d20000885>

Author(s)

Chia-Ling Chen, Ernesto Lopez, Yung-Joon Jung, Sinan Müftü, Selvapraba Selvarasah, and Mehmet R. Dokmeci

Mechanical and electrical evaluation of parylene-C encapsulated carbon nanotube networks on a flexible substrate

Chia-Ling Chen,¹ Ernesto Lopez,² Yung-Joon Jung,² Sinan Müftü,² Selvaprabha Selvarasah,¹ and Mehmet R. Dokmeci^{1,a)}

¹Department of Electrical and Computer Engineering, Northeastern University, Boston, Massachusetts 02115, USA

²Department of Mechanical and Industrial Engineering, Northeastern University, Boston, Massachusetts 02115, USA

(Received 18 June 2008; accepted 7 August 2008; published online 4 September 2008)

Carbon nanotube networks are an emerging conductive nanomaterial with applications including thin film transistors, interconnects, and sensors. In this letter, we demonstrate the fabrication of single-walled carbon nanotube (SWNT) networks on a flexible polymer substrate and then provide encapsulation utilizing a thin parylene-C layer. The encapsulated SWNT network was subjected to tensile tests while its electrical resistance was monitored. Tests showed a linear-elastic response up to a strain value of 2.8% and nearly linear change in electrical resistance in the 0%–2% strain range. The networks' electrical resistance was monitored during load-unload tests of up to 100 cycles and was hysteresis-free. © 2008 American Institute of Physics. [DOI: 10.1063/1.2976633]

Carbon nanotube (CNT) networks are excellent candidates for flexible electronic devices and sensors due to their strength, flexibility, and the attractive properties provided by the nanotubes. Nanotube networks are fabricated utilizing either high temperature chemical vapor deposition or room temperature solution based deposition methods (preferred for applications on polymeric substrates) that include spray coating, dip coating, drop casting, and transfer printing. The development of cost-effective, simple, and large scale fabrication approaches coupled with the emerging nanotube applications greatly enhanced the popularity of CNT networks. Zhao *et al.*¹ and Grüner² demonstrated CNT-network based chemical and biological sensors, whereas Hur *et al.*³ and Gui *et al.*⁴ demonstrated applications of networks in transistors and biological sensors. Furthermore, Snow *et al.*^{5–7} demonstrated gas and chemical sensors utilizing nanotube networks. A recent review paper of Grüner details the fabrication and applications of these nanomaterials.⁸ Furthermore, the fabrication of nanotube networks on polymeric substrates^{9,10} is expected to have applications in the emerging field of flexible electronics as electrical interconnects and devices and as strain sensors in wearable/smart textiles. Despite the advances in nanotube network based devices, the mechanical properties of nanotube networks on flexible media are not investigated. Furthermore, prior to translation of this nanomaterial into a product of technological importance, another crucial requirement is the need for proper encapsulation technology for protecting the nanomaterial from the environmental factors such as humidity, corrosion, and dust particles.

The commonly used substrate materials for flexible electronics include polymers such as poly(ethylene naphthalate),¹¹ poly(ethylene terephthalate),¹² and polydimethylsiloxane.¹³ These polymers are commercially available at low cost, yet most are only available in a sheet form, and being flexible, they are not readily compatible with microfabrication technologies. In addition, they are hundreds

of microns in thickness and hence are bulky. The bending rigidity of thin films is proportional to Et^3 , where E is the elastic modulus and t is the thickness of the film.¹⁴ Therefore, thinner substrates may be preferable since they can be readily rolled into cylinders with a smaller diameter without causing any damage to the materials. Here, we introduce a flexible polymeric substrate material, namely, poly(paraxylylene) (parylene-C), which is deposited at room temperature, compatible with microfabrication processes, and, while attached onto a substrate during the fabrication process, can be readily peeled off after the completion of the device. In addition, parylene-C is transparent, does not react with most chemicals, and is sufficiently flexible and durable, which enables its use as a substrate with thicknesses down to 10 μm . In this letter, we present a technology for the fabrication and encapsulation of nanotube networks on a flexible polymeric substrate, and then we evaluate the electrical behavior of the fabricated structure under various mechanical loading conditions.

Highly purified HiPCo-grown single-walled CNTs (SWNTs) (diameter of ~ 1 –2 nm and 2–5 μm in length) suspended in an aqueous solution (Nantero, Woburn, MA) were utilized to fabricate the nanotube networks on the flexible parylene-C substrate, as shown in Fig. 1(a). The fabrication process is described in Fig. 1(b) and starts by depositing a thin (10 μm) parylene-C (PDS 2010 Parylene-C Deposition System, SCS, Indianapolis, IN, USA) layer on a 3" silicon wafer. Then, Au contact pads (1500 Å) are selectively deposited utilizing a shadow mask. An aqueous solution of SWNTs was next drop cast onto the parylene-C substrate and the sample was left to dry in air. For encapsulation, a 10 μm thick conformal, transparent, and pinhole-free parylene-C layer was deposited at room temperature to protect the SWNT network from the environment. Contact areas for electrical measurements were next etched on the top parylene-C layer utilizing an inductively coupled plasma etcher (Plasmatherm 790) with oxygen plasma. A 2000 Å thick aluminum hard mask was utilized during the dry etch step, which was removed right after the etch. After fabrica-

^{a)}Author to whom correspondence should be addressed. Electronic mail: mehmetd@ece.neu.edu.

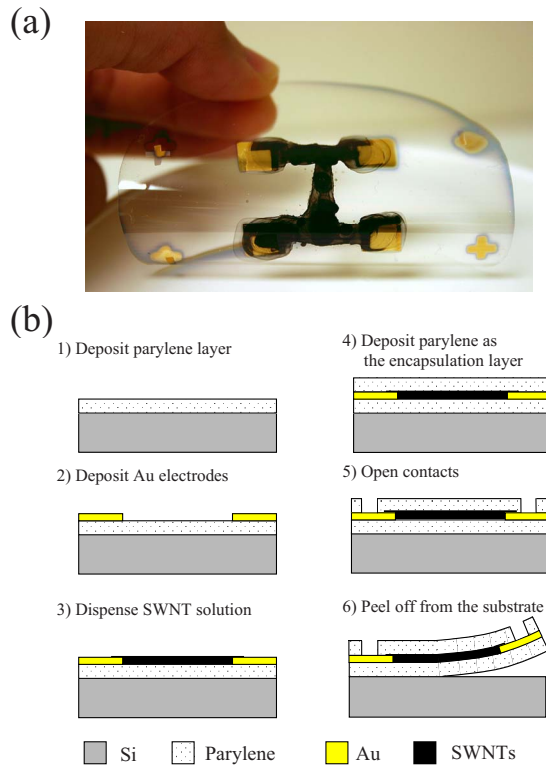


FIG. 1. (Color online) (a) Optical photograph of the flexible SWNT network. (b) Fabrication sequence starts by (1) depositing a parylene-C ($10\ \mu\text{m}$) layer onto silicon substrate, (2) sputtering a thin ($1500\ \text{\AA}$) layer of metal (Au) onto the parylene-C layer, (3) drop casting an aqueous solution of SWNTs onto the parylene layer, (4) depositing the top parylene-C layer to encapsulate the network, (5) opening contact areas over the Au electrodes, and (6) peeling off the flexible network from the silicon substrate.

tion, the flexible SWNT network was peeled off from the silicon wafer and is ready for testing.

Parylene-C as-deposited has a hydrophobic surface (water contact angle of 98°),¹⁵ and the drop casting process results in SWNTs to dry on the surface in a random orientation [Fig. 2(a)] forming a SWNT network. The van der Waals interactions between the closely packed nanotubes hold the network together, and connections between nanotubes allow electrical conductivity.¹⁶ The CNT network is attached to the polymer substrate (parylene-C) through van der Waals forces and possibly through chemical bonds.¹⁷

The bulk deformation behavior of the encapsulated SWNT network on a parylene-C substrate was next characterized in a tensile test. A schematic of the $20\ \mu\text{m}$ thick specimen is shown in Fig. 2(b), where the test area was $2 \times 10\ \text{mm}^2$. The specimen was then suspended horizontally and reinforced by gluing $250\ \mu\text{m}$ thick cardboards on both sides of the sample [Fig. 2(c)]. This particular “dog bone” design ensured that the normal strain was confined to the test area. The strain distribution was computed by finite element analysis (FEA) using ANSYS (Canonsburg, PA). More than 30 000 “Solid 185” elements were used to model the system. The results in Fig. 2(c) show that the horizontal sections of the specimen experience approximately 1/1000th of the strain experienced in the vertical section. Through this design, the impact of film deformation near the gold pads was kept at a minimum during the tensile testing of the SWNT network.

The tensile testing was carried out by using a universal testing machine UMT-2 (CETR, Campbell, CA) with a strain

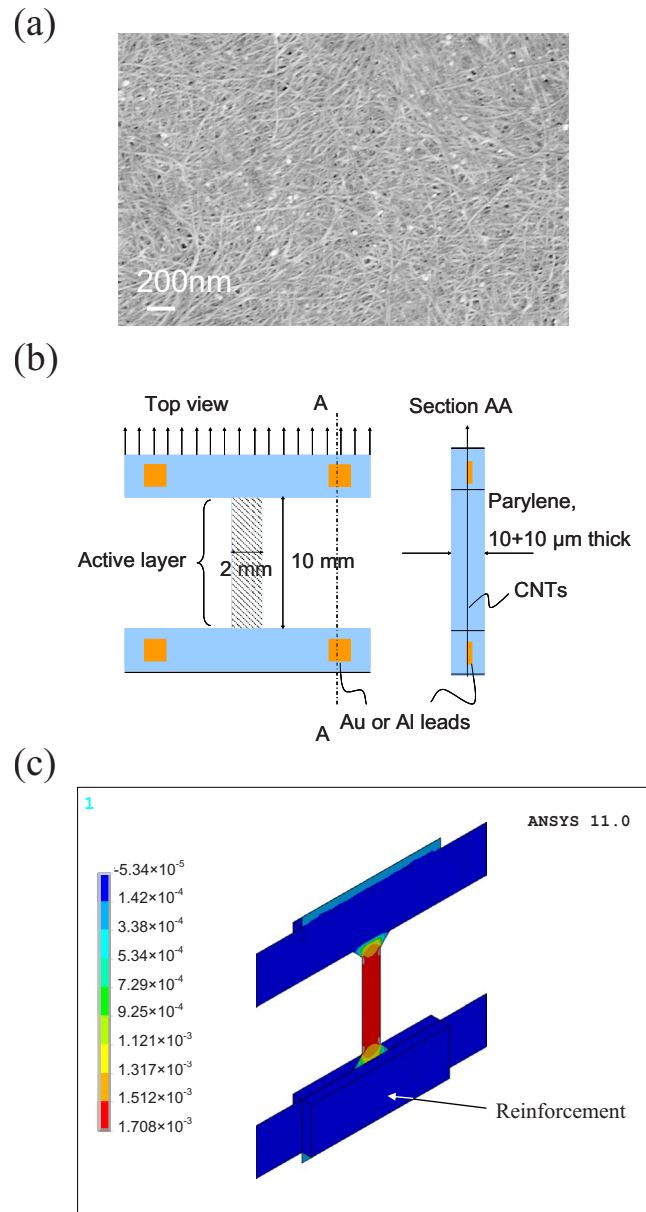


FIG. 2. (Color online) (a) Scanning electron microscopy micrograph of the SWNTs deposited on the parylene-C substrate. (b) The dimensions of the tested sample with a test area of $2 \times 10\ \text{mm}^2 \times 20\ \mu\text{m}$. (c) Strain distribution in the test specimen by FEA. This particular dog bone design ensured that the normal strain was confined to the test area.

rate of $0.2\ \text{mm/min}$. Parylene-C is a crystalline polymer with a glass transition temperature of $90\ ^\circ\text{C}$. The tests conducted at room temperature and with the slow strain rate ensured that the transient effects of this viscoelastic material did not influence the deformation behavior. The normal stress, $\sigma = F/A_0$, was calculated based on the applied force, F , and the cross sectional area ($A_0 = 40 \times 10^{-9}\ \text{m}^2$) of the specimen. The normal strain, $\varepsilon = (L - L_0)/L_0$, was calculated based on the initial length of $L_0 = 10\ \text{mm}$ and the final length, L . The measured stress-strain curve for the encapsulated SWNT network is displayed in Fig. 3(a). As seen in Fig. 3(a), a linear-elastic response ($\sigma = E\varepsilon$) was observed from the SWNT network until the proportional strain limit (ε_{PL}) of 2.8%. The modulus of elasticity (E) of the encapsulated SWNT network was measured as 1.93 GPa (based on three samples) with a standard deviation of 0.08 GPa.

The initial two-terminal electrical resistance (R_0) of the encapsulated SWNT network ($2\ \text{mm} \times 10\ \text{mm} \times 20\ \mu\text{m}$)

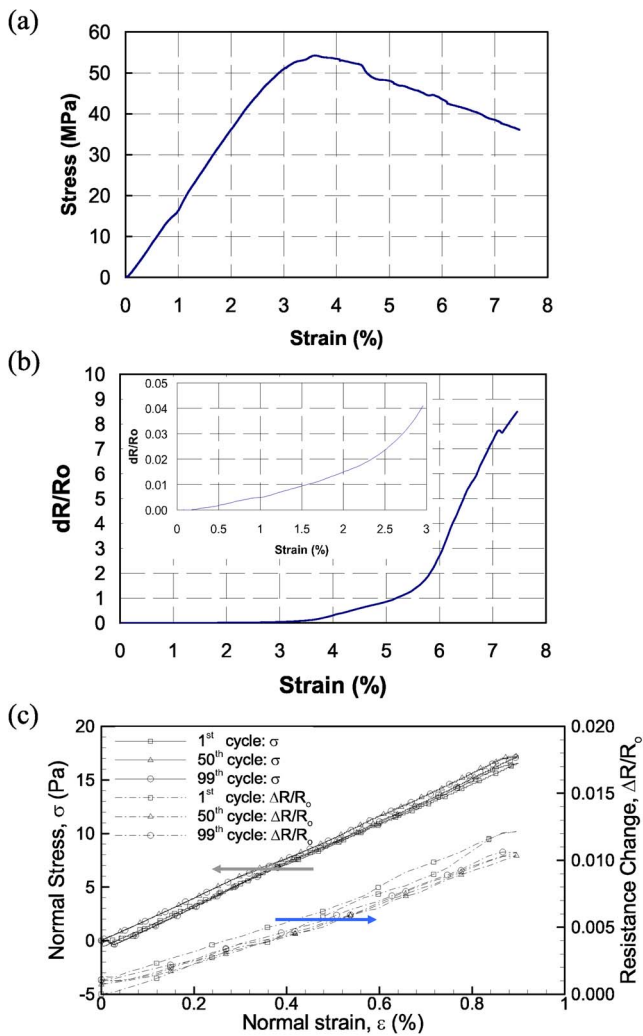


FIG. 3. (Color online) (a) The normal stress vs strain from the tensile testing of the encapsulated SWNT network on the parylene-C substrate with a strain rate of 0.2 mm/min. The proportional strain limit (ϵ_{PL}) was measured to be 2.8%. (b) Measured change in resistance (normalized to initial resistance) vs strain. The details of 0%–3% strain range are magnified in the inset. (c) Normal stress vs normal strain and the measured change in resistance (normalized to initial resistance) vs normal strain after the first, 50th, and 99th loading cycles.

was 66 Ω . The change in resistance was normalized with respect to the initial resistance ($\Delta R/R_0$) and is plotted as a function of the imposed normal strain (ϵ) in Fig. 3(b). The details of the 0%–3% strain range are magnified in the inset of Fig. 3(b). This figure indicates that the rate of change in resistance with respect to strain, ($d\Delta R/d\epsilon$), is nearly linear until reaching a strain value of 2%, where $\Delta R/R_0=1.5\%$. The rate of resistance change increases precipitously thereafter, and at 3% strain the $\Delta R/R_0$ became 4%. Beyond the linear-elastic range ($\epsilon > 2.8\%$), the resistance corresponding to larger values of strain changed even more rapidly, and the resistance of the SWNT network increased to about 800% at failure ($\epsilon_{fail} \cong 7.5\%$).

We believe that parylene dominates the deformation of the system, and the CNT network conforms to the deformation of the parylene substrate. The loosely bound nanotubes in the network, in response to the elongation, tend to separate from each other, hence the resistance of the network increases. Beyond the elastic region, this movement accelerates, hence causing the resistance to increase precipitously.

We next examined the loading behavior of the SWNT network by performing cyclic testing for 100 times in the 0%–0.9% strain range. Figure 3(c) shows the normal stress (σ) and the change in resistance ($\Delta R/R_0$) in the specimen as a function of normal strain (ϵ) for the first, 50th, and the 99th cycles. While the σ – ϵ curve displayed a very small amount of hysteresis for the first loading cycle, the 99th loading cycle was nearly hysteresis-free. This figure shows very similar results for the $(\Delta R/R_0)$ – ϵ behavior during the cyclic loading test, where a small amount of hysteresis is observed for the first cycle and nearly none is observed for the last 99th loading cycle. The fact that the resistance of the SWNT network remained nearly hysteresis-free during the mechanical loading cycles implies that the nanotube network has potential applications in flexible electronics. The SWNT network remained conductive until the end of 100 cycles when the testing was concluded. The load-unload testing was repeated with a higher maximum strain ($\epsilon=0$ to 2%) and the measured resistance was also nearly hysteresis-free.

The encapsulated SWNT network is a mechanically robust, flexible, and conductive nanomaterial that may find potential applications as lateral interconnects in flexible media, wearable/smart textiles, and, after taking advantage of parylene micromachining, can be readily turned into flexible strain sensors.

This research was conducted at the George J. Kostas Nanoscale Technology and Manufacturing Research Center at Northeastern University. The authors would like to thank Prashanth Makaram and Professor Ahmed Busnaina for providing the SWNTs. Kindly acknowledge funding from the Office of the Provost at NEU and the NSF (NSEC) Center for High-rate Nanomanufacturing.

- ¹Y.-L. Zhao, L. Hu, J. F. Stoddart, and G. Gruner, *Adv. Mater.* (Weinheim, Ger.) **9999**, 1 (2008).
- ²G. Gruner, *Anal. Bioanal. Chem.* **384**, 322 (2006).
- ³S.-H. Hur, O. O. Park, and J. A. Rogers, *Appl. Phys. Lett.* **86**, 243502 (2005).
- ⁴E.-L. Gui, L.-J. Li, P. S. Lee, A. Lohani, S. G. Mhaisalkar, Q. Cao, S. J. Kang, J. A. Rogers, N. C. Tansil, and Z. Gao, *Appl. Phys. Lett.* **89**, 232104 (2006).
- ⁵E. S. Snow, J. P. Novak, P. M. Campbell, and D. Park, *Appl. Phys. Lett.* **82**, 2145 (2003).
- ⁶E. S. Snow, J. P. Novak, M. D. Lay, E. H. Houser, F. K. Perkins, and P. M. Campbell, *J. Vac. Sci. Technol. B* **22**, 1990 (2004).
- ⁷E. S. Snow, F. K. Perkins, E. J. Houser, S. C. Badesco, and T. L. Reinecke, *Science* **307**, 1942 (2005).
- ⁸G. Gruner, *J. Mater. Chem.* **16**, 3533 (2006).
- ⁹Y. J. Jung, S. Kar, S. Talapatra, C. Soldano, G. Viswanathan, X. Li, Z. Yao, F. S. Ou, A. Avadhanula, R. Vajtai, S. Curran, O. Nalamasu, and P. M. Ajayan, *Nano Lett.* **6**, 413 (2006).
- ¹⁰E. Artukovic, M. Kaempgen, D. S. Hecht, S. Roth, and G. Gruner, *Nano Lett.* **5**, 757 (2005).
- ¹¹T. Sekitani, Y. Kato, S. Iba, H. Shinaoka, T. Someya, T. Sakurai, and S. Takagi, *Appl. Phys. Lett.* **86**, 073511 (2005).
- ¹²E. Menard, R. G. Nuzzo, and J. A. Rogers, *Appl. Phys. Lett.* **86**, 093507 (2005).
- ¹³J. Kang, J. Lee, T. H. Kim, J. Park, M.-J. Seong, and S. Hong, *Nanotechnology* **19**, 135305 (2008).
- ¹⁴S. P. Timoshenko and S. Woinowsky-Krieger, *Theory of Plates and Shells* (McGraw-Hill, New York, 1959).
- ¹⁵S. Selvarasah, S.-H. Chao, C.-L. Chen, S. Sridhar, A. Busnaina, A. Khademhosseini, and M. R. Dokmeci, *Sens. Actuators, A* **145-146**, 306 (2008).
- ¹⁶T. Hertel, R. E. Walkup, and P. Avouris, *Phys. Rev. B* **58**, 13870 (1998).
- ¹⁷L. S. Schadler, S. C. Giannaris, and P. M. Ajayan, *Appl. Phys. Lett.* **73**, 3842 (1998).